Average vector field methods for the coupled Schrödinger–KdV equations*

Zhang Hong(张 弘)[a], Song Song-He(宋松和)[a)b)†], Chen Xu-Dong(陈绪栋)[a], and Zhou Wei-En(周炜恩)[a]

[a] Department of Mathematics and System Science, College of Science, National University of Defense Technology, Changsha 410073, China
[b] State Key Laboratory of High Performance Computing, National University of Defense Technology, Changsha 410073, China

(Received 13 November 2013; revised manuscript received 8 January 2014; published online 15 May 2014)

The energy preserving average vector field (AVF) method is applied to the coupled Schrödinger–KdV equations. Two energy preserving schemes are constructed by using Fourier pseudospectral method in space direction discretization. In order to accelerate our simulation, the split-step technique is used. The numerical experiments show that the non-splitting scheme and splitting scheme are both effective, and have excellent long time numerical behavior. The comparisons show that the splitting scheme is faster than the non-splitting scheme, but it is not as good as the non-splitting scheme in preserving the invariants.

Keywords: coupled Schrödinger–KdV equations, average vector field method, splitting method, Fourier pseudospectral method

PACS: 02.60.Cb, 02.70.Bf, 02.30.Jr **DOI:** 10.1088/1674-1056/23/7/070208

1. Introduction

Nonlinear phenomena play a crucial role in applied mathematics and physics, many of which can be modeled by the coupled partial differential equations, for example, KdV–mKdV equations, KdV–ZK equations, KdV–Burgers equations, and Schrödinger–KdV equations.[1] In this paper we consider one of the coupled Schrödinger–KdV equations (CSKE)[2]

$$\begin{cases} \mathrm{i}\epsilon E_t + \dfrac{3}{2}E_{xx} - \dfrac{1}{2}NE = 0, \quad (x,t) \in R \times (0,T], \\ N_t + \dfrac{N_{xxx}}{2} + \dfrac{1}{2}(N^2 + |E|^2)_x = 0, \quad (x,t) \in R \times (0,T], \end{cases} \tag{1}$$

with the initial value and periodic boundary conditions of

$$\begin{aligned} &E(x,t) = E(x+l,t), \quad N(x,t) = N(x+l,t), \\ &(x,t) \in R \times (0,T], \\ &E(x,0) = E_0(x), \quad N(x,0) = N_0(x), \end{aligned} \tag{2}$$

where $E_0(x)$ and $N_0(x)$ are known l-periodic functions, $l > 0$, E is a complex function describing the electric field of Langmuir oscillations, N is a real function describing low-frequency density perturbation, and $\epsilon > 0$ is a constant. In the CSKE (1), the first equation is called the electric field equation and the second is the density equation. The initial value and periodic boundary condition problem for the CSKE (1) has the following invariants:[2]

(i) number of Langmuir plasmons:

$$I_1(t) = \int_\Omega |E|^2 \mathrm{d}x = \int_\Omega |E_0|^2 \mathrm{d}x = I_1(0), \quad t \geq 0, \tag{3}$$

(ii) number of particles:

$$I_2 = \int_\Omega N \mathrm{d}x = \int_\Omega N_0 \mathrm{d}x = I_2(0), \quad t \geq 0, \tag{4}$$

(iii) oscillation energy:

$$\begin{aligned} I_3 &= \int_\Omega 3|E_x|^2 + |E|^2 N + \frac{N^3}{3} - \frac{1}{2}(N_x)^2 \mathrm{d}x \\ &= I_3(0), \quad t \geq 0. \end{aligned} \tag{5}$$

In numerical simulation these invariants can be used to test the conservation properties of the schemes.

This problem has drawn much attention for decades and has motivated a series of studies in physics and mathematics. The analytical solutions of the CSKE have been studied in Refs. [3]–[7]. Recently, several methods have been proposed to solve the CSKE (1). Abdou *et al.*[8] introduced a variational iteration method for the CSKE, Kaya[1] developed a decomposition method, and Labidi *et al.*[9] applied the ansatz method to solve this problem. In order to give numerical solutions for the CSKE, Appert *et al.*[2] used the explicit three-time-level Zabusky–Kruskal scheme for the density equation and a standard Crank–Nicholson scheme for the electric field equation, Bai *et al.*[10] proposed the finite–element method (FEM) for the CSKE, Golbabai *et al.*[11] used the radial basis function method, and Liu *et al.*[12] studied an element-free Galerkin method to solve the CSKE.

For the PDEs which have such invariants, it is widely believed that structure preserving methods, for example, numerical methods that preserve the invariants, generally yield qualitatively better numerical results,[13] in recent years much

*Project supported by the National Natural Science Foundation of China (Grant No. 91130013) and the Open Foundation of State Key Laboratory of High Performance Computing of China.

†Corresponding author. E-mail: shsong@nudt.edu.cn

© 2014 Chinese Physical Society and IOP Publishing Ltd

work has been devoted to finding unified frameworks. For example, Furihata[14] proposed the discrete variational derivative (DVD) method, Celledoni *et al.*[15] proposed the average vector field (AVF) method in difference context, Matsuo[16] proposed the discrete partial derivative (DPD) method in finite element context, and Yaguchi *et al.*[17] proposed four conservative numerical schemes based on the Hamiltonian structure and the variational structure of the PDEs. To our best knowledge, only Bai *et al.*[10] proposed a finite–element method to preserve invariants of the CSKE (1). Therefore, it is still very challenging to develop an energy preserving scheme for the CSKE.

This paper is organized as follows. In Section 2, we describe the average vector field method. In Section 3, the average vector field method is applied to the Hamiltonian form of the CSKE and the non-splitting and splitting schemes are constructed. In order to make a comparison, we also give a symplectic Fourier pseudospectral scheme of the Hamiltonian form (14). In Section 4, numerical experiments of the CSKE are presented to show the effectiveness of the proposed average vector field methods. Section 5 ends with conclusion.

2. Average vector field method

Many evolution PDEs, such as the KdV equation, can be written as infinite Hamiltonian systems of the form[18]

$$\dot{u} = D\frac{\delta H}{\delta u}, \tag{6}$$

where u depends on $(x,t) \in R^{\mathrm{d}} \times R$, u belongs to a Hilbert space $\mathscr{B}$ with values $u(x,t) \in R^m$, D is a constant linear differential operator, and $\dot{u} = \partial u/\partial t$. For example, if $d = m = 1$, $\mathscr{B} = L^2(\Omega)$, the Hamiltonian $\mathscr{H}$ and the variational derivative are

$$\mathscr{H}[u] = \int_\Omega H(x;u,u_x,u_{xx},\ldots)\,\mathrm{d}x, \tag{7}$$

$$\frac{\delta \mathscr{H}}{\delta u} = \frac{\partial H}{\partial u} - \partial_x\left(\frac{\partial H}{\partial u_x}\right) + \partial_x^2\left(\frac{\partial H}{\partial u_{xx}}\right) - \cdots, \tag{8}$$

where Ω is a subset of $R \times R$, and u satisfies $u|_{\partial\Omega} = 0$.

When D is a skew-adjoint operator, we denote it by $\boldsymbol{S}$. We use a suitable way to discretize $\boldsymbol{S}$ and the Hamiltonian $\mathscr{H}$ in space direction. Let $L = x_{\mathrm{R}} - x_{\mathrm{L}}$ be the length of the interval $[x_{\mathrm{L}}, x_{\mathrm{R}}]$, then discretize it by uniform grids with a space step size of $\Delta x = L/N$, where N is the number of nodes. We denote the finite discretization of x and u by $\bar{x} = [x_0, x_1, \ldots, x_{N-1}]$ and $\bar{u} = [u_0, u_1, \ldots, u_{N-1}]$, then we obtain the semi-discrete system

$$\bar{u}_t = \bar{\boldsymbol{S}}\nabla\bar{\mathscr{H}}(\bar{u}), \quad \bar{u} \in R^N. \tag{9}$$

Here, $\bar{\boldsymbol{S}}$ is the $N \times N$ skew-symmetric structure matrix corresponding to $\boldsymbol{S}$, $\bar{\mathscr{H}}\Delta x$ is an approximation to $\mathscr{H}$, and the variational derivative $(\delta/\delta u)(\bar{\mathscr{H}}\Delta x)$ is given by $\nabla\bar{\mathscr{H}}$.

References [15] and [19] have proved that the average vector field method preserves the Hamiltonian $\mathscr{H}$. This is an extension of the implicit middle point method. The average vector field integrator of (9) has the form of

$$\frac{\bar{u}^{n+1} - \bar{u}^n}{\Delta t} = \int_0^1 \bar{\boldsymbol{S}}\nabla\bar{\mathscr{H}}((1-\tau)\bar{u}^n + \tau\bar{u}^{n+1})\,\mathrm{d}\tau. \tag{10}$$

Reference [15] proved that

$$\bar{\mathscr{H}}(\bar{u}^{n+1}) = \bar{\mathscr{H}}(\bar{u}^n). \tag{11}$$

For $\dot{\bar{u}} = \bar{\boldsymbol{S}}\nabla\bar{\mathscr{H}}(\bar{u})$, we have

$$\dot{\bar{\mathscr{H}}} = (\nabla\bar{\mathscr{H}})^{\mathrm{T}}\bar{\boldsymbol{S}}\nabla\bar{\mathscr{H}} = 0. \tag{12}$$

Hence, $\bar{\mathscr{H}}$ is preserved by the flow of $\dot{u} = \bar{\boldsymbol{S}}\nabla\bar{\mathscr{H}}(u)$.

3. Numerical schemes

3.1. The non-splitting scheme

The CSKE (1) can be written by decomposing $E = p + \mathrm{i}q$ in real and imaginary components as

$$\begin{cases} \epsilon p_t = -\dfrac{3}{2}q_{xx} + \dfrac{1}{2}Nq, \\ N_t = -\dfrac{1}{2}N_{xxx} - \dfrac{1}{2}(p^2+q^2+N^2)_x, \\ \epsilon q_t = \dfrac{3}{2}p_{xx} - \dfrac{1}{2}Np, \end{cases} \tag{13}$$

as an infinite-dimensional Hamiltonian PDE in the phase space $\boldsymbol{z} = [p, N, q]^{\mathrm{T}}$,

$$\dot{\boldsymbol{z}} = \boldsymbol{S}\frac{\delta\mathscr{H}}{\delta z}, \tag{14}$$

with the Hamiltonian $\mathscr{H}$ and the skew-symmetric operator $\boldsymbol{S}$

$$\begin{aligned} \mathscr{H} &= I_3 \\ &= \int_\Omega 3|E_x|^2 + |E|^2N + \frac{N^3}{3} - \frac{1}{2}(N_x)^2\,\mathrm{d}x \\ &= I_H(0), \quad t \geq 0, \\ \boldsymbol{S} &= \begin{pmatrix} 0 & 0 & \dfrac{1}{4\epsilon} \\ 0 & -\dfrac{1}{2}\partial x & 0 \\ -\dfrac{1}{4\epsilon} & 0 & 0 \end{pmatrix}. \end{aligned} \tag{15}$$

We can find that the Hamiltonian $\mathscr{H}$ is the energy of the oscillations I_3.

In order to discretize the Hamiltonian PDE (14) in space direction, we choose the Fourier pseudospectral method. References [20]– [22] have shown that when the Fourier pseudospectral method is applied to the multi-symplectic form of PDEs, it can preserve the multi-symplectic conservation laws, hence we think that it may also preserve the Hamiltonian energy of (14).

The key point of the Fourier pseudospectral method is to approximate the partial differential operators. Reference [20]

indicated that the Fourier spectral differential matrix $\boldsymbol{D}_k$ can replace the k-order partial differential operator $\partial^k x$. We present D_1 and D_2 as follows:

$$(D_1)_{j+1,l+1} = \begin{cases} \frac{1}{2}(-1)^{j+l}\mu\cot\left(\mu\frac{x_j - x_l}{2}\right), & j \neq l, \\ 0, & j = l, \end{cases}$$

$$(D_2)_{j+1,l+1} = \begin{cases} \frac{1}{2}(-1)^{j+l+1}\mu^2\csc^2\left(\mu\frac{x_j - x_l}{2}\right), & j \neq l, \\ -\mu^2\frac{2(N/2)^2+1}{6}, & j = l, \end{cases}$$

where $j,l = 0,1,\ldots,N-1$, $\mu = 2\pi/L$, L is the length of space interval, and the even integer N is the number of the subintervals. It can be proved that $\boldsymbol{D}_1$ is an $N \times N$ skew-symmetric matrix. For more details, see Ref. [20] and references therein.

Then we can discretize the skew-symmetric matrix $\boldsymbol{S}$ and the Hamiltonian $\mathscr{H}$ as

$$\bar{\boldsymbol{S}} = \begin{pmatrix} 0 & 0 & \frac{1}{4\epsilon}\boldsymbol{I} \\ 0 & -\frac{1}{2}\boldsymbol{D}_1 & 0 \\ -\frac{1}{4\epsilon}\boldsymbol{I} & 0 & 0 \end{pmatrix},$$

$$\begin{aligned} \bar{\mathscr{H}} &= \Delta x \sum_{i=0}^{N-1} (3((D_1\bar{\boldsymbol{p}})_i^2 + (D_1\bar{\boldsymbol{q}})_i^2) \\ &\quad + (p_i^2 + q_i^2)N_i + \frac{N_i^3}{3} - \frac{1}{2}(D_1 N)_i^2), \end{aligned} \tag{16}$$

where $\boldsymbol{I}$ is an $(N \times N)$-dimensional identity matrix. By applying the average vector field method to (14) and using the Fourier pseudospectral method in space direction discretization, we can obtain the scheme

$$\begin{cases} \epsilon\dfrac{\bar{\boldsymbol{p}}^{n+1} - \bar{\boldsymbol{p}}^n}{\Delta t} = -D_2\dfrac{3(\bar{\boldsymbol{q}}^{n+1} + \bar{\boldsymbol{q}}^n)}{4} + \dfrac{\bar{\boldsymbol{q}}^{n+1}\bar{N}^{n+1} + \bar{\boldsymbol{q}}^n\bar{N}^n + (\bar{\boldsymbol{q}}^{n+1}\bar{N}^n + \bar{\boldsymbol{q}}^n\bar{N}^{n+1})/2}{6}, \\ \dfrac{\bar{N}^{n+1} - \bar{N}^n}{\Delta t} = -D_1D_2\dfrac{\bar{N}^{n+1} + \bar{N}^n}{4} - D_1\dfrac{((\bar{N}^{n+1})^2 + \bar{N}^{n+1}\bar{N}^n + (\bar{N}^n)^2)}{6} \\ \qquad\qquad -D_1\dfrac{(\bar{\boldsymbol{p}}^{n+1})^2 + \bar{\boldsymbol{p}}^{n+1}\bar{\boldsymbol{p}}^n + (\bar{\boldsymbol{p}}^n)^2 + (\bar{\boldsymbol{q}}^{n+1})^2 + \bar{\boldsymbol{q}}^{n+1}\bar{\boldsymbol{q}}^n + (\bar{\boldsymbol{q}}^n)^2}{6}, \\ \epsilon\dfrac{\bar{\boldsymbol{q}}^{n+1} - \bar{\boldsymbol{q}}^n}{\Delta t} = D_2\dfrac{3(\bar{\boldsymbol{p}}^{n+1} + \bar{\boldsymbol{p}}^n)}{4} - \dfrac{\bar{\boldsymbol{p}}^{n+1}\bar{N}^{n+1} + \bar{\boldsymbol{p}}^n\bar{N}^n + (\bar{\boldsymbol{p}}^{n+1}\bar{N}^n + \bar{\boldsymbol{p}}^n\bar{N}^{n+1})/2}{6}. \end{cases} \tag{17}$$

Here, we denote $\bar{\boldsymbol{p}}^n = [p_0^n, p_1^n, \ldots, p_{N-1}^n]^{\mathrm{T}}$, $\bar{\boldsymbol{p}}^n\bar{\boldsymbol{p}}^{n+1} = [p_0^n p_0^{n+1}, p_1^n p_1^{n+1}, \ldots, p_{N-1}^n p_{N-1}^{n+1}]^{\mathrm{T}}$, and others are similar, respectively.

Although the fixed point iteration method can be used to solve the nonlinear system (17), the cost of this implicit method has been criticized. Here, we propose a splitting method for the CSKE (1) which can be solved easier and more efficient than (17).

3.2. Splitting scheme

In Ref. [23], a splitting scheme was used to solve the Schrödinger equation. Owing to this elicitation, we can also apply the second-order strang splitting method to (13) by adapting the linear and non-linear splitting

$$z_t = \mathscr{L}z + \mathscr{N}z, \tag{18}$$

where

$$\mathscr{L}z = \begin{pmatrix} 0 & 0 & -\frac{3}{2\epsilon}\partial x^2 \\ 0 & -\frac{1}{2}\partial x^3 & 0 \\ \frac{3}{2\epsilon}\partial x^2 & 0 & 0 \end{pmatrix} \begin{pmatrix} p \\ N \\ q \end{pmatrix},$$

$$\mathscr{N}z = \begin{pmatrix} \frac{1}{2\epsilon}Nq \\ -\frac{1}{2}(p^2 + q^2 + N^2) \\ -\frac{1}{2\epsilon}Np \end{pmatrix}. \tag{19}$$

Then we obtain the linear and non-linear equations as

$$z_t = \mathscr{L}z, \tag{20}$$

$$z_t = \mathscr{N}z. \tag{21}$$

The Hamilton form of Eqs. (20) and (21) can be written as

$$z_t = \boldsymbol{S}\frac{\delta\mathscr{H}_1}{\delta z}, \tag{22}$$

$$z_t = \boldsymbol{S}\frac{\delta\mathscr{H}_2}{\delta z}, \tag{23}$$

where

$$\mathscr{H}_1 = \int 3|E_x|^2 - \frac{1}{2}(N_x)^2\,\mathrm{d}x, \tag{24}$$

$$\mathscr{H}_2 = \int |E|^2 N + \frac{N^3}{3}\,\mathrm{d}x, \tag{25}$$

$$\boldsymbol{S} = \begin{pmatrix} 0 & 0 & \frac{1}{4\epsilon} \\ 0 & -\frac{1}{2}\partial x & 0 \\ -\frac{1}{4\epsilon} & 0 & 0 \end{pmatrix}. \tag{26}$$

By applying the average vector field method to Eqs. (22) and (23), and using the Fourier pseudo-spectral method in space direction, we can obtain the energy preserving average vector field splitting (AVFS) scheme

$$\epsilon\frac{\bar{\boldsymbol{p}}^{n+1}-\bar{\boldsymbol{p}}^{n}}{\Delta t}=-\boldsymbol{D}_2\frac{3(\bar{\boldsymbol{q}}^{n+1}+\bar{\boldsymbol{q}}^{n})}{4},\quad \frac{\bar{N}^{n+1}-\bar{N}^{n}}{\Delta t}=-\boldsymbol{D}_1\boldsymbol{D}_2\frac{\bar{N}^{n+1}+\bar{N}^{n}}{4},\quad \epsilon\frac{\bar{\boldsymbol{q}}^{n+1}-\bar{\boldsymbol{q}}^{n}}{\Delta t}=\boldsymbol{D}_2\frac{3(\bar{\boldsymbol{p}}^{n+1}+\bar{\boldsymbol{p}}^{n})}{4}, \tag{27}$$

and

$$\begin{cases}\epsilon\dfrac{\bar{\boldsymbol{p}}^{n+1}-\bar{\boldsymbol{p}}^{n}}{\Delta t}=\dfrac{\bar{\boldsymbol{q}}^{n+1}\bar{N}^{n+1}+\bar{\boldsymbol{q}}^{n}\bar{N}^{n}+(\bar{\boldsymbol{q}}^{n+1}\bar{N}^{n}+\bar{\boldsymbol{q}}^{n}\bar{N}^{n+1})/2}{6},\\ \dfrac{\bar{N}^{n+1}-\bar{N}^{n}}{\Delta t}=-\boldsymbol{D}_1\dfrac{(\bar{\boldsymbol{p}}^{n+1})^2+\bar{\boldsymbol{p}}^{n+1}\bar{\boldsymbol{p}}^{n}+(\bar{\boldsymbol{p}}^{n})^2+(\bar{\boldsymbol{q}}^{n+1})^2+\bar{\boldsymbol{q}}^{n+1}\bar{\boldsymbol{q}}^{n}+(\bar{\boldsymbol{q}}^{n})^2}{6}-\boldsymbol{D}_1\dfrac{((\bar{N}^{n+1})^2+\bar{N}^{n+1}\bar{N}^{n}+(\bar{N}^{n})^2)}{6},\\ \epsilon\dfrac{\bar{\boldsymbol{q}}^{n+1}-\bar{\boldsymbol{q}}^{n}}{\Delta t}=-\dfrac{\bar{\boldsymbol{p}}^{n+1}\bar{N}^{n+1}+\bar{\boldsymbol{p}}^{n}\bar{N}^{n}+(\bar{\boldsymbol{p}}^{n+1}\bar{N}^{n}+\bar{\boldsymbol{p}}^{n}\bar{N}^{n+1})/2}{6}.\end{cases} \tag{28}$$

In the splitting method, the solution of one subproblem is employed as the initial value of another. We denote the flow of Eqs. (27) and (28) as $\varphi_1(\tau)=\exp(\tau\mathscr{L}u)$ and $\varphi_2(\tau)=\exp(\tau\mathscr{N}u)$, and then we choose the second-order composition method

$$\varphi(\tau)=\varphi_2\left(\frac{\tau}{2}\right)\varphi_1(\tau)\varphi_2\left(\frac{\tau}{2}\right)=\exp\left(\frac{\tau}{2}\mathscr{N}u\right)\exp(\tau\mathscr{L}u)\exp\left(\frac{\tau}{2}\mathscr{N}u\right). \tag{29}$$

The nonlinear system of Eq. (28) can be solved by using the simple fixed point iteration method.

3.3. The symplectic scheme

In Hamiltonian mechanics, it is of great significance to preserve the symplectic or multi-symplectic structure of the Hamiltonian systems. Various symplectic or multi-symplectic approaches have been developed in Refs. [24]–[27]. One standard approach to obtain a symplectic method for an infinite-dimensional Hamiltonian PDE is to first discretize the Hamiltonian PDE in space to obtain a finite-dimensional Hamiltonian system, and then evolve the semi-discrete system in time by symplectic integrators. Here, we use the Fourier pseudospectral method to discretize the Hamiltonian system (14) in space and the implicit midpoint rule with respect to time, and then the following symplectic Fourier pseudospectral (SFP) scheme can be obtained as

$$\begin{cases}\epsilon\dfrac{\bar{\boldsymbol{p}}^{n+1}-\bar{\boldsymbol{p}}^{n}}{\Delta t}=-\boldsymbol{D}_2\dfrac{3(\bar{\boldsymbol{q}}^{n+1}+\bar{\boldsymbol{q}}^{n})}{4}+\dfrac{\bar{\boldsymbol{q}}^{n+1}\bar{N}^{n+1}+\bar{\boldsymbol{q}}^{n}\bar{N}^{n}+\bar{\boldsymbol{q}}^{n+1}\bar{N}^{n}+\bar{\boldsymbol{q}}^{n}\bar{N}^{n+1}}{8},\\ \dfrac{\bar{N}^{n+1}-\bar{N}^{n}}{\Delta t}=-\boldsymbol{D}_1\boldsymbol{D}_2\dfrac{\bar{N}^{n+1}+\bar{N}^{n}}{4}-\boldsymbol{D}_1\dfrac{((\bar{N}^{n+1})^2+2\bar{N}^{n+1}\bar{N}^{n}+(\bar{N}^{n})^2)}{8}\\ \qquad\qquad -\boldsymbol{D}_1\dfrac{(\bar{\boldsymbol{p}}^{n+1})^2+2\bar{\boldsymbol{p}}^{n+1}\bar{\boldsymbol{p}}^{n}+(\bar{\boldsymbol{p}}^{n})^2+(\bar{\boldsymbol{q}}^{n+1})^2+2\bar{\boldsymbol{q}}^{n+1}\bar{\boldsymbol{q}}^{n}+(\bar{\boldsymbol{q}}^{n})^2}{8},\\ \epsilon\dfrac{\bar{\boldsymbol{q}}^{n+1}-\bar{\boldsymbol{q}}^{n}}{\Delta t}=\boldsymbol{D}_2\dfrac{3(\bar{\boldsymbol{p}}^{n+1}+\bar{\boldsymbol{p}}^{n})}{4}-\dfrac{\bar{\boldsymbol{p}}^{n+1}\bar{N}^{n+1}+\bar{\boldsymbol{p}}^{n}\bar{N}^{n}+\bar{\boldsymbol{p}}^{n+1}\bar{N}^{n}+\bar{\boldsymbol{p}}^{n}\bar{N}^{n+1}}{8}.\end{cases} \tag{30}$$

In the next section we will compare the non-splitting and splitting schemes with this SF scheme.

4. Numerical experiments

In this section, we present some numerical examples to show the accuracy and effectiveness of the proposed methods (17), (27), and (28). These examples are also provided in Refs. [1], [2], [10], and [12] and have been integrated by the Crank–Nicolson (CN) method, the finite-element method, and the element free Galerkin (EFG) method.

In the following, we will compare the AVF and AVFS schemes with the SFP scheme. In addition, we use the fixed-point iteration method to solve the nonlinear schemes (17), (28), and (30). The accuracies of the AVF, AVFS, and SFP schemes are tested by using the error norm L_2 and L_∞

$$L_2=\|u-\bar{u}\|_2=\left(\Delta x\sum_{j=0}^{N-1}(u_j-\bar{u}_j)^2\right)^{1/2}, \tag{31}$$

$$L_\infty=\|u-\bar{u}\|_\infty=\max_{0\le j\le N-1}|u_j-\bar{u}_j|, \tag{32}$$

where Δx is the space step size, N is the number of points, u is the exact solution, and $\bar{u}$ is the numerical solution.

Example 1 A stationary traveling localized solution of the CSKE (1) can be given by[28]

$$E(x,t)=-\frac{6}{5}\sqrt{3}\alpha\,\mathrm{sech}(\xi)\tanh(\xi)\times\exp\left(\mathrm{i}\alpha\left(\frac{3}{20\epsilon}-\frac{\epsilon\alpha}{6}\right)t-\frac{\epsilon x}{3}\right), \tag{33}$$

$$N(x,t) = -\frac{9}{5}\alpha \mathrm{sech}^2(\xi), \tag{34}$$

where $\xi = (\alpha/10)^{1/2}(x+\alpha t)$, and α is a free positive parameter.

We take the value of the exact solution (33) and (34) at $t = 0$ as our initial conditions

$$E_0 = -\frac{6}{5}\sqrt{3}\alpha \mathrm{sech}(\xi)\tanh(\xi)\exp\left(\mathrm{i}\alpha\left(-\frac{\epsilon x}{3}\right)\right), \tag{35}$$

$$N_0 = -\frac{9}{5}\alpha \mathrm{sech}^2(\xi), \tag{36}$$

where $\epsilon = 1$, $\alpha = 0.45$, and $\xi = (\alpha/10)^{1/2}x$.

To test the AVF scheme and the AVFS scheme, we choose a time step $\Delta t = 0.01$, a space interval $[-30, 30]$, and a space step size $\Delta x = 0.5$. We compute the solutions to $t = 1$. The numerical results for the CSKE (1) with initial conditions (35) and (36) are shown in Figs. 1 and 2. From these two figures, we can see that both the AVF sheme and the AVFS scheme perform well. In addition, these results are the same as that obtained by Ref. [12].

In order to show the accuracies of the two methods, we compute the numerical solutions to $t = 10$ with $\Delta t = 0.1$, and $\Delta x = 0.5$. The comparisons of L_2 and L_∞ errors between the AVF scheme, AVFS scheme, and the SFP scheme are shown in Table 1. From this table we can see that the two energy preserving schemes have almost the same accuracy as the SFP scheme, and the AVF scheme is a little better than the AVFS scheme.

The corresponding errors of the three invariant I_1, I_2, and I_3 for the two proposed methods and the SFP method are also shown in Figs. 3–5. From these figures, we can see that the AVF, AVFS, and SFP schemes preserve the number of Langmuir plasmons, the number of particles, and the energy of the oscillations, the SFP scheme is better than the AVF and AVFS schemes in preserving the invariant I_1. Nevertheless, compared with the AVFS scheme, the AVF scheme performs better in preserving the global invariants.

Table 1. Comparison of L_2 and L_∞ errors for the numerical solutions at $t = 10$, $\Delta t = 0.1$, and $\Delta x = 0.5$.

Method	Error	p	q	N
SFP	L_2	7.1295×10^{-3}	7.7965×10^{-3}	3.3059×10^{-4}
	L_∞	2.9475×10^{-3}	5.9897×10^{-3}	1.1302×10^{-4}
AVF	L_2	7.1292×10^{-3}	7.7966×10^{-3}	3.2685×10^{-4}
	L_∞	2.9475×10^{-3}	5.9895×10^{-3}	1.1297×10^{-4}
AVFS	L_2	7.1598×10^{-3}	7.8143×10^{-3}	5.0509×10^{-4}
	L_∞	2.9902×10^{-3}	6.0078×10^{-3}	1.7098×10^{-4}

Table 2 shows the CPU time and the numerical errors at $t = 10$, which are all implemented in Matlab 2010b on a personal computer (CPU: Intel(R) I5 2520, 2.5 GHz, RAM: 8 GB). We can see that the AVFS scheme has the same accuracy as the the AVF scheme, but is more efficient than the AVF scheme.

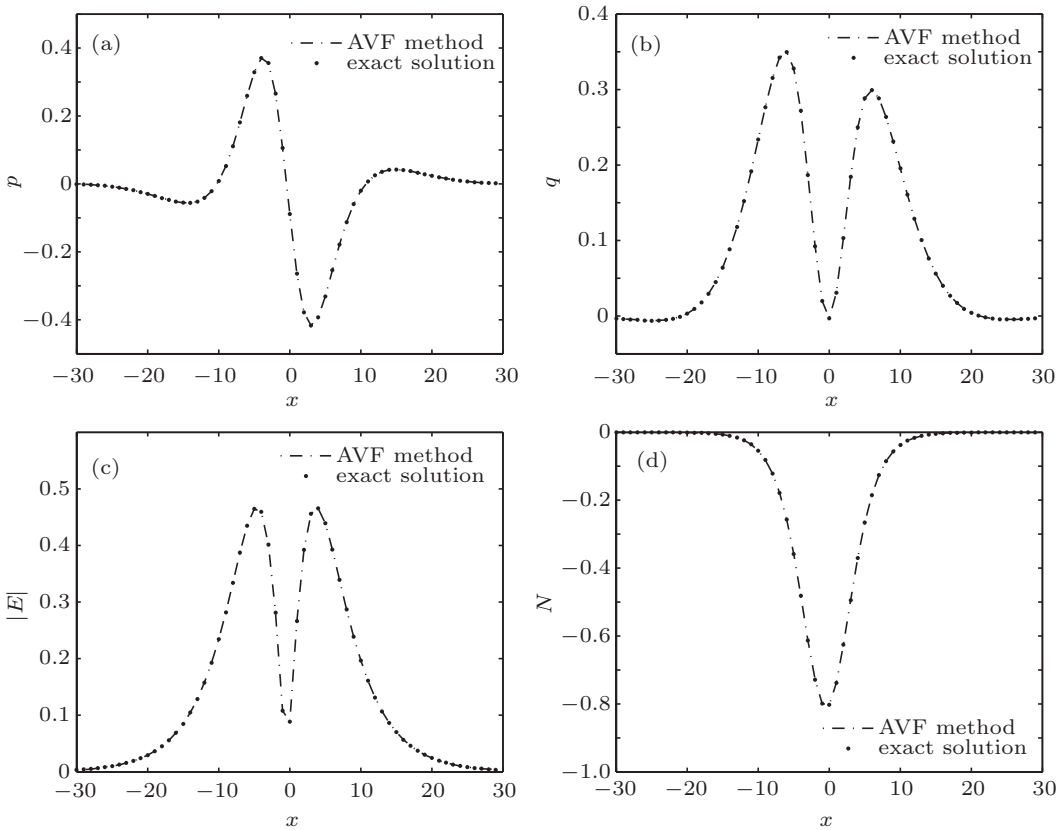


Fig. 1. Numerical solutions of the AVF scheme and exact solutions at $t = 1$, $\Delta t = 0.01$, and $\Delta x = 0.5$. (a) p–x, (b) q–x, (c) $|E|$–x, and (d) N–x.

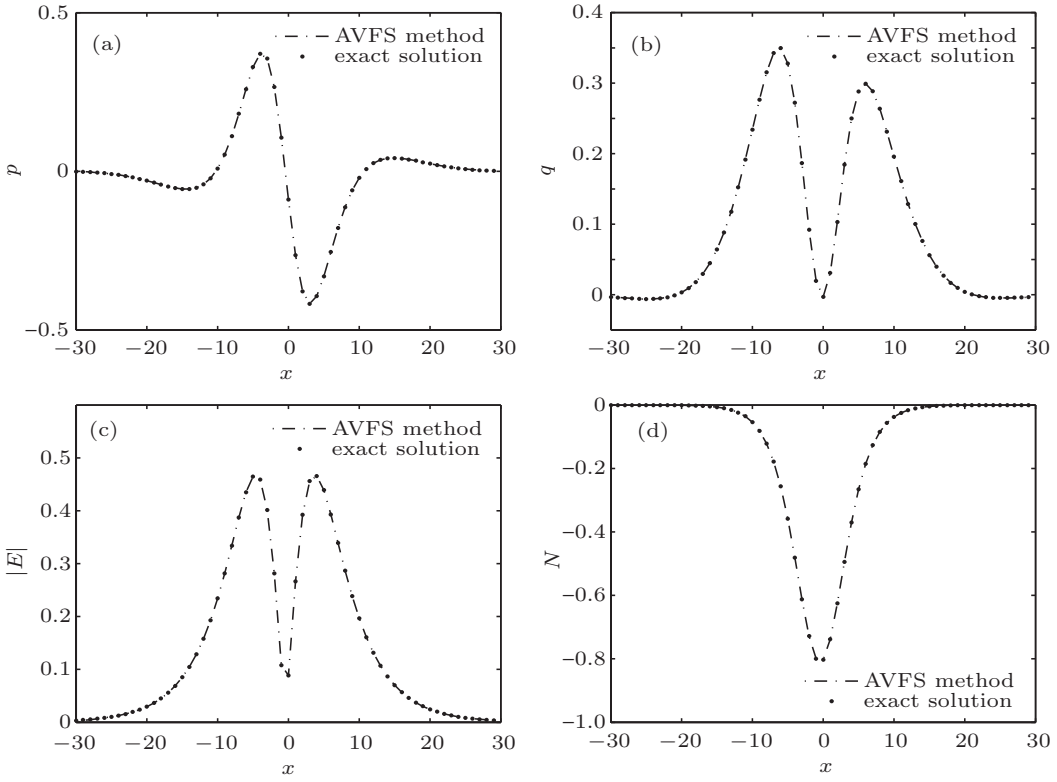


Fig. 2. Numerical solutions of the AVFS scheme and exact solutions at $t = 1$, $\Delta t = 0.01$, and $\Delta x = 0.5$. (a) p–x, (b) q–x, (c) $|E|$–x, and (d) N–x.

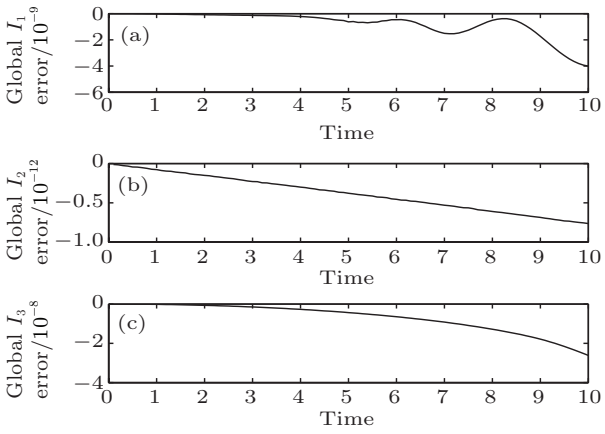


Fig. 3. Global errors of (a) I_1, (b) I_2, and (c) I_3 obtained by the AVF scheme at $t = 10$, $\Delta t = 0.1$, and $\Delta x = 0.5$.

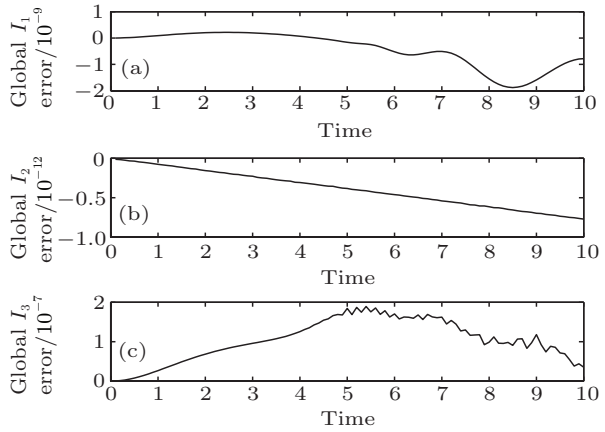


Fig. 4. Global errors of (a) I_1, (b) I_2, and (c) I_3 obtained by the AVFS scheme at $t = 10$, $\Delta t = 0.1$, and $\Delta x = 0.5$.

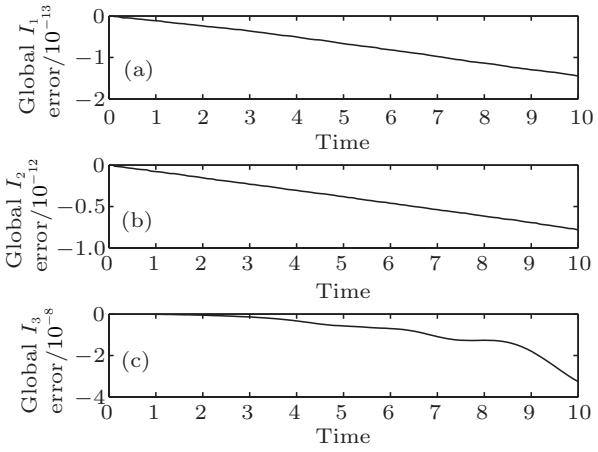


Fig. 5. Global errors of (a) I_1, (b) I_2, and (c) I_3 obtained by the SFP scheme at $t = 10$, $\Delta t = 0.1$, and $\Delta x = 0.5$.

Table 2. Comparison of CPU time (in units of s) and L_2 errors between the AVF and AVFS schemes from $t = 0$ to $t = 10$.

Method	AVF	L_2 error of N	AVFS	L_2 error of N
$\Delta t = 0.1, \Delta x = 0.5$	0.7543	3.2685×10^{-4}	0.2386	5.0509×10^{-4}
$\Delta t = 0.1, \Delta x = 0.25$	3.2751	2.9604×10^{-4}	0.7671	4.5821×10^{-4}
$\Delta t = 0.01, \Delta x = 0.5$	4.5601	3.6671×10^{-4}	0.9698	3.6568×10^{-4}
$\Delta t = 0.01, \Delta x = 0.25$	19.7027	3.2043×10^{-4}	2.7464	3.3157×10^{-4}

Example 2 In this example, we consider the CSKE in the following form:[12]

$$\begin{cases} \mathrm{i}E_t = E_{xx} + NE, \\ N_t + 6NN_x + N_{xxx} = (|E|^2)_x. \end{cases} \tag{37}$$

The initial and boundary conditions are the same as Eq. (2). In Ref. [29], Fan gave the exact solutions

$$E(x,t) = \mathrm{e}^{\mathrm{i}\theta}(-\sqrt{2}(2c_2 \pm \delta) + 6\sqrt{2}c_2 \mathrm{sech}^2(\sqrt{c_2}\xi)), \quad (38)$$

$$N(x,t) = -\frac{1}{3}(\gamma + 6c_2 \pm \delta) + 6c_2 \mathrm{sech}^2(\sqrt{c_2}\xi), \quad (39)$$

where $\xi = x + 2\gamma t$, $\theta = \gamma x + (\gamma + 3\gamma^2 \pm \delta)t/3$, and $\delta = \sqrt{\sqrt{2}c_1 c_3 + 4c_2^2}$. The c_1, c_3, and $c_2 > 0$ are arbitrary constants. For simplicity, $c_1 = c_3 = 0$ are used. For the CSKE (37), the first two invariants are the same as I_1 and I_2, but the third invariant is

$$I_3' = \int \frac{1}{2}\left(-|E_x|^2 + |E|^2 N + \frac{1}{4}N_x^2 - \frac{N^3}{2}\right) \mathrm{d}x. \quad (40)$$

First, we give the Hamiltonian form of the CSKE (37) with state variable $\boldsymbol{z} = [p, N, q]^{\mathrm{T}}$, and the Hamiltonian function and the skew-symmetric operator are

$$\mathscr{H} = \int \frac{1}{2}\left(-p_x^2 - q_x^2 + (p^2 + q^2)N + \frac{1}{4}N_x^2 - \frac{N^3}{2}\right) \mathrm{d}x,$$

$$\boldsymbol{S} = \begin{pmatrix} 0 & 0 & 1 \\ 0 & 2\partial x & 0 \\ -1 & 0 & 0 \end{pmatrix}. \quad (41)$$

Applying the AVF integrator to the CSKE (37), we can obtain the scheme

$$\begin{cases} \dfrac{\bar{\boldsymbol{p}}^{n+1} - \bar{\boldsymbol{p}}^n}{\Delta t} = \boldsymbol{D}_2 \dfrac{\bar{\boldsymbol{q}}^{n+1} + \bar{\boldsymbol{q}}^n}{2} + \dfrac{\bar{\boldsymbol{q}}^{n+1}\bar{N}^{n+1} + \bar{\boldsymbol{q}}^n \bar{N}^n + (\bar{\boldsymbol{q}}^{n+1}\bar{N}^n + \bar{\boldsymbol{q}}^n \bar{N}^{n+1})/2}{3}, \\ \dfrac{\bar{N}^{n+1} - \bar{N}^n}{\Delta t} = -\boldsymbol{D}_1((\bar{N}^{n+1})^2 + \bar{N}^{n+1}\bar{N}^n + (\bar{N}^n)^2) - \boldsymbol{D}_1\boldsymbol{D}_2 \dfrac{\bar{N}^{n+1} + \bar{N}^n}{2} \\ \qquad\qquad + \boldsymbol{D}_1 \dfrac{(\bar{\boldsymbol{p}}^{n+1})^2 + \bar{\boldsymbol{p}}^{n+1}\bar{\boldsymbol{p}}^n + (\bar{\boldsymbol{p}}^n)^2 + (\bar{\boldsymbol{q}}^{n+1})^2 + \bar{\boldsymbol{q}}^{n+1}\bar{\boldsymbol{q}}^n + (\bar{\boldsymbol{q}}^n)^2}{3}, \\ \dfrac{\bar{\boldsymbol{q}}^{n+1} - \bar{\boldsymbol{q}}^n}{\Delta t} = -\boldsymbol{D}_2 \dfrac{\bar{\boldsymbol{p}}^{n+1} + \bar{\boldsymbol{p}}^n}{2} - \dfrac{\bar{\boldsymbol{p}}^{n+1}\bar{N}^{n+1} + \bar{\boldsymbol{p}}^n \bar{N}^n + (\bar{\boldsymbol{p}}^{n+1}\bar{N}^n + \bar{\boldsymbol{p}}^n \bar{N}^{n+1})/2}{3}. \end{cases} \quad (42)$$

In this example, we only test the AVF scheme and the computations are done with a time step $\Delta t = 0.01$, a space interval $[-30, 30]$, and a space step size $\Delta x = 0.25$. In Fig. 6, we present the evolution of the numerical solutions of p, q, $|E|$, and N, from $t = 0$ to $t = 1$ with $c_2 = 0.01$ and $\gamma = 0.1$. In Fig. 7, we plot the corresponding absolute errors of the invariants I_1, I_2, and I_3'. In Fig. 8, we show the numerical solutions obtained by the AVF scheme with $c_2 = 0.01$ and $\gamma = 1$. In Fig. 9, we plot the corresponding errors of the invariants from $t = 0$ to $t = 1$.

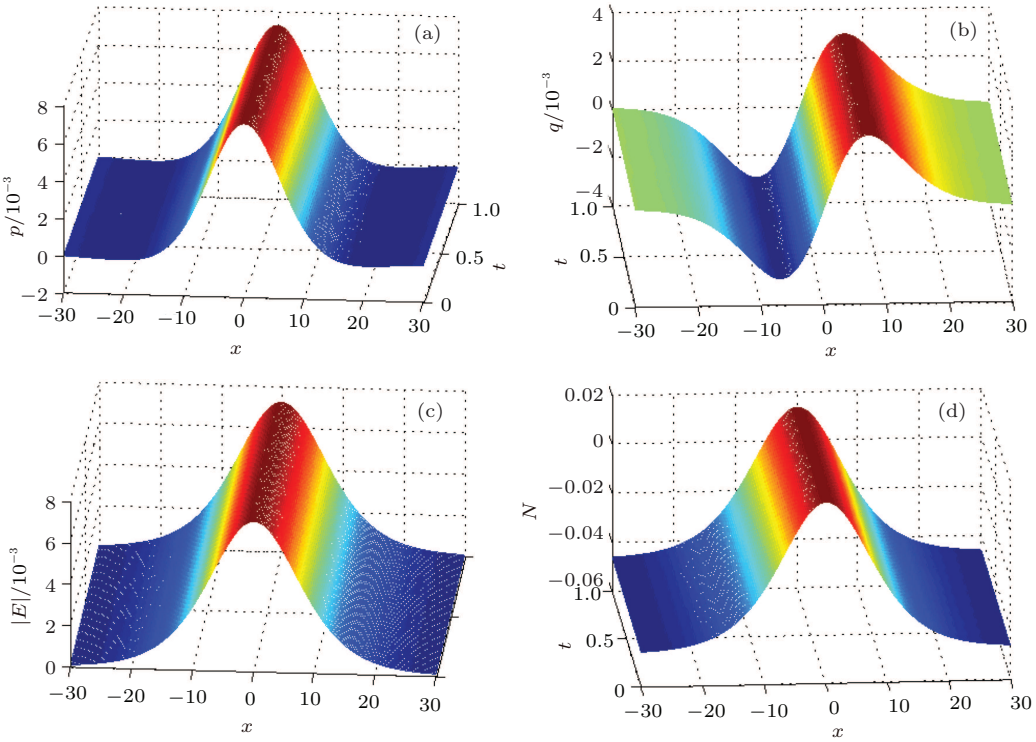


Fig. 6. (color online) Evolution of the AVF solutions ((a) p, (b) q, (c) $|E|$, and (d) N) from $t = 0$ to $t = 1$, $\Delta t = 0.01$, $\Delta x = 0.25$, $c_2 = 0.01$, and $\gamma = 0.1$.

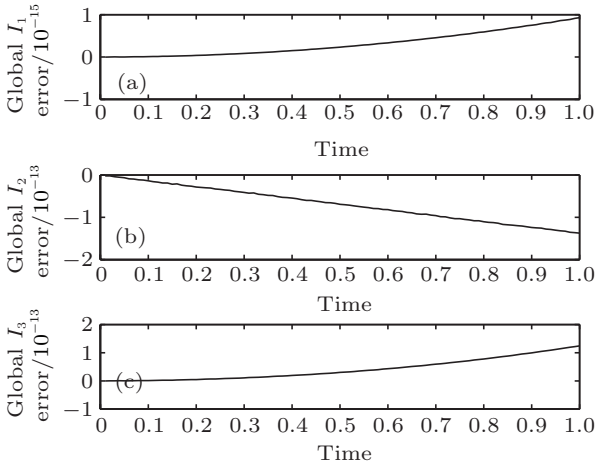


Fig. 7. Global errors of (a) I_1, (b) I_2, and (c) I_3' obtained by the AVF scheme, from $t = 0$ to $t = 1$, $\Delta t = 0.01$, $\Delta x = 0.25$, $c_2 = 0.01$, and $\gamma = 0.1$

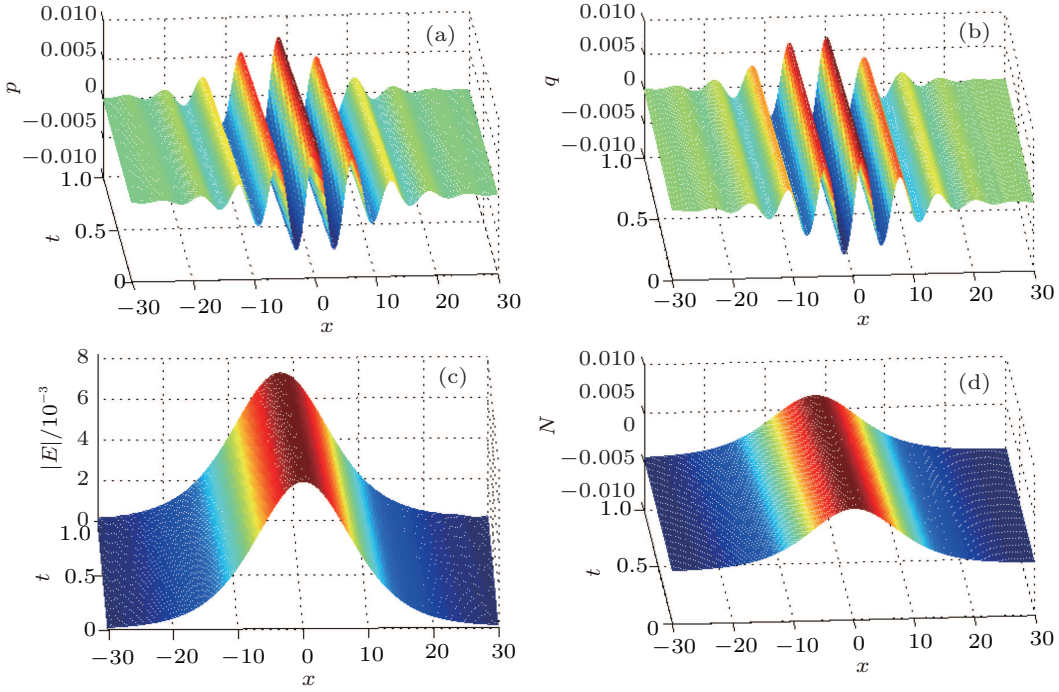


Fig. 8. (color online) Evolution of the AVF solutions ((a) p, (b) q, (c) $|E|$, and (d) N) from $t = 0$ to $t = 1$, $\Delta t = 0.01$, $\Delta x = 0.25$, $c_2 = 0.01$, and $\gamma = 1$.

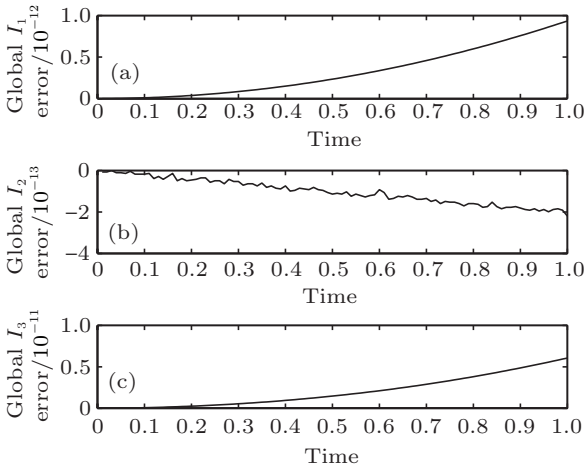


Fig. 9. Global errors of (a) I_1, (b) I_2, and (c) I_3' obtained by the AVF scheme, from $t = 0$ to $t = 1$, $\Delta t = 0.01$, $\Delta x = 0.25$, $c_2 = 0.01$, and $\gamma = 1$.

From Figs. 6–9 we can find that the AVF scheme preserves the three invariants globally and the numerical solutions do not oscillate.

5. Conclusions

In this paper, we propose two energy-preserving methods to solve the CSKE. From the results of numerical experiments, we can see that both the AVF method and the AVFS method are effective. The AVF method, nevertheless, has better performance in preserving the three discrete invariants. However, the AVFS method is much more efficient than the AVF method under the same spatial grids.

References

[1] Kaya D 2003 *Phys. Lett. A* **313** 82
[2] Appert K and Vaclavik J 1977 *Phys. Fluids* **20** 1845
[3] Nishikawa K, Hojo H, Mima K and Ikeze H 1974 *Phys. Rev. Lett.* **33** 148
[4] Mahankov V G 1978 *Phys. Rep.* **35** 1
[5] Gibbous J 1977 *J. Plasma Phys.* **17** 153
[6] Albert J and Pava J A 2003 *Proc. R. Soc.* **133** 987
[7] Peng Y Z 2004 *Pramana* **62** 933
[8] Abdou M A and Sdiman A A 2005 *Physica D* **211** 1
[9] Labidi M, Ebadi G, Zerrad E and Biswas A 2012 *Pramana* **78** 59
[10] Bai D and Zhang L 2009 *Phys. Lett. A* **373** 2237
[11] Golbabai A and Safdari-Baighani A 2011 *Computing* **92** 225
[12] Liu Y Q, Cheng R J and Ge H X 2013 *Chin. Phys. B* **22** 100204
[13] Miyatake Y, Yaguchi T and Matsuo T 2012 *J. Comput. Phys.* **231** 4542
[14] Furihata D 1999 *J. Comput. Phys.* **156** 181
[15] Celledoni E, Grimm V, McLachlan R I, RcLaren D I, O'Neale D, Owren B and Quispel G R W 2012 *J. Comput. Phys.* **231** 6770
[16] Matsuo T 2008 *J. Comput. Appl. Math.* **218** 506
[17] Yaguchi T, Matsuo T and Sugihara M 2010 *J. Comput. Appl. Math.* **234** 1036
[18] Olver P J 2000 *Applications of Lie Groups to Differential Equations* (Vol. 107) (Berlin: Springer-Verlag)
[19] Hairer E 2010 *JNAIAM* **5** 73
[20] Chen J b, Qin M Z and Tang Y F 2002 *Comput. Math. Appl.* **43** 1095
[21] Chen Y M, Song S H and Zhu H J 2011 *J. Comput. Appl. Math.* **236** 1354
[22] Qian X, Song S H, Gao E and Li W B 2012 *Chin. Phys. B* **21** 070206
[23] Weideman J A C and Herbst B M 1986 *SIAM J. Numer. Anal.* **23** 485
[24] Feng K, Wu H M, Qin M Z and Wang D L 1989 *J. Comput. Math.* **7** 71
[25] McLachlan R I 1994 *Numer. Math.* **66** 462
[26] Tang Y F 1994 *Comput. Math. Appl.* **27** 31
[27] Hu W P and Deng Z C 2008 *Chin. Phys. B* **17** 3923
[28] Guo B and Shen L 1982 *Proceedings of DD-3 Symposium,* August 23–September 16, 1982 Changchun, China, p. 417
[29] Fan E G 2002 *J. Phys. A: Math. Gen.* **35** 6853